

High spin states of ^{86}Zr

E. K. Warburton, C. J. Lister,* J. W. Olness, P. E. Haustein, S. K. Saha, and D. E. Alburger
Brookhaven National Laboratory, Upton, New York 11973

J. A. Becker

Lawrence Livermore Laboratory, Livermore, California 94550

R. A. Dewberry† and R. A. Naumann

Departments of Physics and Chemistry, Princeton University, Princeton, New Jersey 08540

(Received 15 November 1984)

The level scheme of ^{86}Zr was studied by in-beam measurements on γ transitions in the $^{60}\text{Ni}(^{29}\text{Si},2\text{pn}\gamma)^{86}\text{Zr}$ reaction and by helium-jet studies of delayed γ -ray activity from the $^{58}\text{Ni}(^{32}\text{S},3\text{pn})^{86}\text{Nb}(\beta^+/\text{EC})^{86}\text{Zr}$ reaction. In the latter study, measurements consisted of γ - γ and β - γ coincidences, excitation functions, and a lifetime determination. An ^{86}Nb decay scheme was obtained which suggests $J^\pi=5^+$ for the ^{86}Nb ground state. The in-beam study consisted of γ - γ coincidences, excitation functions, angular distributions, and lifetime measurements via both Doppler shift attenuation and recoil distance methods. The high-spin decay scheme and level lifetimes obtained from the in-beam studies suggest intrinsic modes of excitation rather than the collective behavior seen in ^{84}Zr .

I. INTRODUCTION

The study reported herein is part of an effort to understand the high-spin spectroscopy of the even Zr isotopes from ^{82}Zr (Ref. 1) to ^{90}Zr (Ref. 2), that is, from one end of the $g_{9/2}$ neutron shell to the other. A quite detailed and careful in-beam study of ^{86}Zr was recently made by Hattula *et al.*³ using $\text{Sr}(^3\text{He},x\text{n})$ and $\text{Sr}(^4\text{He},x\text{n})$ reactions. Some previous but less comprehensive studies have also been reported.⁴⁻⁸ It was anticipated that the production of ^{86}Zr via a heavy-ion reaction, such as $^{29}\text{Si}+^{60}\text{Ni}$, would both enhance the population of high spin states and provide favorable conditions for measuring level lifetimes through the recoil distance method (RDM). In practice, the decay scheme was not extended beyond a probable $J^\pi=14^+$ state at 6321 keV, possibly due to the fragmentation of the decay pattern into many cascades. However, the extraction of lifetime information for many of the levels has provided a new insight into the structure of these states.

The low-lying high-spin states of the even Zr isotopes can be studied also via the β^+/EC decay of the corresponding Nb isotopes. Previous studies of ^{86}Nb decay have been made, most recently by Korschinek *et al.*⁵ and Della Negra *et al.*⁹ It was felt that further decay measurements would yield valuable data supplementing the in-beam results, and so, such a study was also undertaken.

II. PROCEDURES AND RESULTS

A. $^{86}\text{Nb}(\beta^+/\text{EC})^{86}\text{Zr}$

The ^{86}Nb radioactivity measurements were performed at the Brookhaven National Laboratory (BNL) double MP tandem facility using a helium-jet system¹⁰ whose use for

other spectroscopic studies in this mass region has been described previously.¹¹⁻¹³ Sources of ^{86}Nb were prepared with high yield by the $^{58}\text{Ni}(^{32}\text{S},3\text{pn})^{86}\text{Nb}$ reaction at $E(^{32}\text{S})=130-150$ MeV. Efficient transport of this activity in the helium-jet system allowed measurements of excitation functions, lifetimes, x-ray and γ -ray energies and intensities, and the accumulation of (x,γ,t) , (γ,γ,t) , and (β,γ,t) coincidence spectra.

A decay scheme for $^{86}\text{Nb}(\beta^+/\text{EC})^{86}\text{Zr}$ was constructed from these data. Use was also made of data from the in-beam study to be described in Sec. II B. Relative intensities observed for the γ rays assigned to ^{86}Nb decay and the placement of the γ rays in the ^{86}Nb decay scheme are given in Table I, while the decay scheme is shown in Fig. 1. There is strong overlap between the decay scheme established for ^{86}Nb decay and the in-beam $\text{Sr}(^3\text{He},x\text{n}\gamma)^{86}\text{Zr}$ study of Hattula *et al.*³ They observed all the ^{86}Zr levels we observed except the top two at 3254 and 3418 keV and the lower-lying member of the 3030-keV doublet. The evidence that there are two rather than one 3030-keV levels is twofold. (1) The 388-keV $3418\rightarrow 3030$ transition is in coincidence with the 1363-keV γ ray, but not the 988-keV γ ray; (2) the 3030-keV level produced in the in-beam studies of Ref. 3 and the present work (Sec. II B) emits 360- and 1363-keV γ rays, but not a 988-keV γ ray.

Once the ^{86}Nb decay scheme had been established, a separate series of experiments was performed to measure the decay energy of ^{86}Nb . These experiments involved (β^+,γ) coincidence spectroscopy in which positrons gated by selected γ rays were detected in a plastic scintillator telescope, consisting of a thin (1 mm) ΔE detector in front of a thick (15 cm) E detector, positioned at 180° with respect to the $\text{Ge}(\text{Li})$ γ -ray detector. Positrons entering the telescope from the ^{86}Nb source passed through a thin Mylar window when exiting the helium-jet system. Pro-

TABLE I. ^{86}Zr energy levels deduced from the assignment of γ rays to the β^+ /EC decay of ^{86}Nb .

$J^{\pi a}$	E_i^b (keV)	E_f (keV)	E_γ^c (keV)	I_γ^d (relative)	BR ^c (%)
2 ⁺	751.744(30)	0	751.740(30)	1000(25)	100
2 ⁺	1421.764(50) ^f	752	670.013(40)	152(7)	87(2)
		0	1421.66(20)	23(3)	13(2)
4 ⁺	1666.599(60)	752	914.810(50)	799(17)	100
(3 ⁺)	2041.896(90) ^f	1667	(375.335)	< 6	< 6
		1422	620.111(90)	78(4)	79(3)
		752	1290.30(30)	21(3)	21(3)
(3 ⁻)	2343.740(60) ^f	2042	(301.844)	< 7	< 8
		1667	677.20(10)	25(4)	29(4)
		1422	921.960(60)	62(5)	71(4)
		752	(1591.980)	< 7	< 8
6 ⁺	2669.806(80)	1667	1003.240(50)	382(9)	100
5 ⁻	2705.609(70)	1667	1039.037(30) ^g	65(20)	100
[5] ^h	3016.857(80)	2706	311.248(30)	14(2)	100
	3029.47(13) ^{i,j}	2042	987.569(90)	52(5)	100
	3029.545(90) ⁱ	2670	359.718(40)	17(2)	15(2)
		1667	1363.134(60)	93(6)	85(2)
	3254.30(10) ^j	3030	(224.642)	< 5	< 3
		2670	584.520(56)	100(3)	53(2)
		1667	1587.75(10)	90(6)	47(2)
	3417.644(90) ^j	3254	(163.344)	< 3	< 2
		3030	388.13(15) ^k	55(5) ^k	34(3)
		2670	747.755(90)	66(6)	40(3)
		1667	1751.14(20)	42(3)	26(2)

^aFrom Ref. 3 unless otherwise noted.

^bCorrected for recoil. The numbers in parentheses are the uncertainties in the least significant figure.

^cNot corrected for recoil. Energies in parentheses are inferred from the level separation. The energies are obtained from both the delayed and in-beam studies.

^dIf multiplied by 8.90 these units are the same as those of Table IV.

^eThe level branching ratio in percent.

^fObserved in the in-beam ($^3\text{He}, x\text{n}\gamma$) study of Ref. 3 but not in the present in-beam ($^{29}\text{Si}, 2\text{pn}\gamma$) study.

^gDoublet with a $^{84}\text{Y}(\beta^+/\text{EC})\gamma$ ray. Separated in the multiscaled singles data and in the in-beam study.

^hFrom the in-beam study and the formation of this level in $\text{Nb}(\beta^+)$.

ⁱThe evidence that there is an energy level doublet near 3029.5 keV is discussed in the text.

^jNot observed in either in-beam studies, i.e., ($^3\text{He}, x\text{n}\gamma$) or ($^{29}\text{Si}, 2\text{pn}\gamma$).

^kCorrected for an ^{87}Y activity.

cedures used have been described fully.¹¹ The telescope was calibrated with well-known positron emitters, e.g., ^{27}Si , ^{39}Ca , ^{58}Cu , and ^{63}Zn . These were produced in the helium-jet system and transported and counted in an identical geometry as the ^{86}Nb sources. In addition, $^{42}\text{Sc}^m$ —produced in ^{32}S bombardment of ^{12}C and/or ^{16}O contaminants—provided a convenient internal calibration. End point energies were analyzed by two independent methods: Fermi-Kurie analysis and use of shape-fitting functions.¹⁴ Identical results within experimental errors were obtained by these methods. Table II displays end point energies for the three most intense γ -ray gates. Since the decay scheme of ^{86}Nb is complex (see Fig. 1), the method of analysis used is approximate and the measured end point must be associated with an effective excitation energy which we take to be the weighted mean as determined from the γ and β^+ intensities of Fig. 1. The uncertainty associated with this procedure is the main contribution to the final adopted Q_{EC} of 8150(200) keV. β^+ spectra in coincidence with the nine next most intense

γ -ray peaks of Table I were also extracted. The results for these were consistent with the analysis just described; however, the statistics were not good enough to give comparable accuracy.

A value of Q_{EC} of 7980(80) keV was extracted by Della Negra *et al.*⁹ from similar β - γ and (recoil ^{86}Zr)- β coincidence measurements. However, this result was based on the assumption (erroneous) that 100% of the β^+ feeding was into the 2670-keV level. The actual measured end points were in good agreement with the present results (Table II) and a treatment based on the decay scheme of Fig. 1 would presumably yield a Q_{EC} value in agreement with the present result.

The half-life of ^{86}Nb was investigated by multiscale 4096-channel γ spectra in five equally spaced time bins. Three measurements were made with time bins of 1, 20, and 100 s, respectively. The decays of all the identified γ rays (Table I) were followed and all had half-lives consistent with that determined from the three most intense γ rays, namely 87.8 ± 0.5 s (statistical errors only). Selected

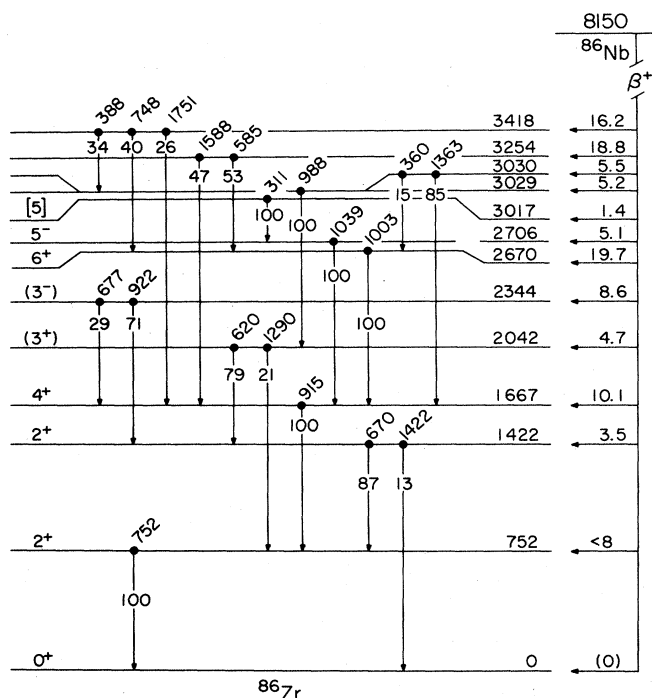


FIG. 1. Decay scheme for $^{86}\text{Nb}(\beta^+/\text{EC})^{86}\text{Zr}$. The γ - and β^+/EC -branching ratios (given in percent) are from Tables I and III, respectively. The spin-parity assignments are those of Ref. 3.

decays are illustrated in Fig. 2. This verification gives added credence to the decay scheme of Fig. 1. A total systematic uncertainty of ~ 1 s is assumed in the half-life measurements so that the adopted value is $t_{1/2} = 88(1)$ s. This value is in good agreement with the value of 87(3) s obtained by Della Negra *et al.*⁹

The intensities of Table I translate into the β^+/EC branching ratios of Table III. Note that these branching ratios have asymmetric uncertainties, (σ_+/σ_-) . The upper uncertainty is statistical only, while the lower uncertainty σ_- includes an estimate of the effect of missing γ -ray flux. As is often the case in complicated β -decay schemes, it is difficult to ascertain and communicate the uncertainty in β -decay branching ratios due to the probably significant but unobserved γ -ray flux from higher-lying levels. If the β decay populated a high-lying level which had a complicated γ decay, then appreciable γ flux

TABLE II. Measured positron end points and Q_{EC} values for ^{86}Nb decay.

Gating transition (keV)	$E_{\beta^+}^{\text{max}}$ (keV)	Q_{EC}^{a} (keV)	Q_{EC} adopted (keV)
752	4254(140)	8096	
916	4264(130)	8106	
1003	4202(280)	8235	8150(200)

^aCalculated from the weighted average for the final ^{86}Zr excitation energy (see the text).

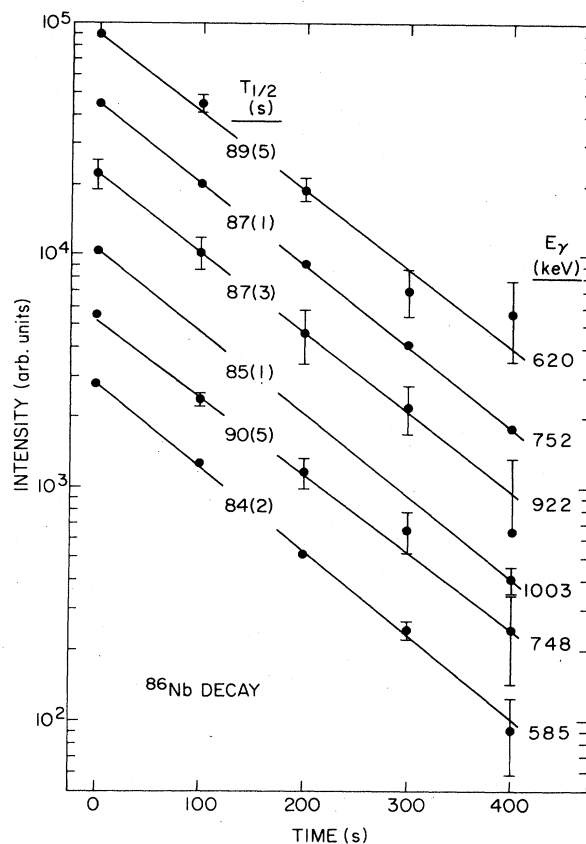


FIG. 2. Time decay of γ rays following $^{86}\text{Nb}(\beta^+/\text{EC})^{86}\text{Zr}$. Some data points are omitted for clarity.

TABLE III. Branching ratios and allowed $\log ft$ values for $^{86}\text{Nb}(\beta^+/\text{EC})^{86}\text{Zr}$. Calculated using $t_{1/2} = 88(1)$ s and $Q_{\text{EC}} = 8150(200)$ keV.

^{86}Zr	E_x (keV)	$\beta^+/\text{EC}^{\text{b}}$	
		Branching ratio (%)	$\log ft$
2^+	752	<8	>6.9
2^+	1422	3.5(9/22)	7.02(13)
4^+	1667	10.1(16/35)	6.47(14)
(3^+)	2042	4.7(7/21)	6.66(11)
(3^-)	2344	8.6(7/15)	6.28(10)
6^+	2670	19.7(15/23)	5.76(10)
5^-	2706	5.1(20/28)	6.35(20)
[5]	3017	1.4(2/21)	6.76(12)
[4]	3029	5.2(6/20)	6.19(12)
[5]	3030	5.5(9/22)	6.16(13)
[5]	3254	18.8(12/21)	5.52(12)
[5]	3418	16.2(11/22)	5.50(12)

^aThe spin-parity assignments in square brackets are speculations based on the β^+/EC - and γ -decay modes, the other assignments are from Ref. 3.

^bFrom the relative intensities of Table I. The numbers in parentheses give the asymmetric uncertainties (σ_+/σ_-) . σ_+ is the purely statistical uncertainty while σ_- incorporates an estimate of the possible effects of undetected γ -ray feedings from higher-lying levels, as explained in the text. The uncertainty assigned to the $\log ft$ values corresponds to σ_+ .

TABLE IV. ^{86}Zr energy levels, lifetimes, and γ -ray transitions deduced from $^{60}\text{Ni}(^{29}\text{Si}, 2\text{pn}\gamma)^{86}\text{Zr}$.

J^π a	E_i^b (keV)	E_f (keV)	E_γ^c (keV)	I_γ	Angular distribution ^d A_2 (%)	A_4 (%)	I_f^e ($\times 10^{-2}$)	τ_f^f (ps)
2^+	751.744(30)	0	751.740(30)	10560(120)	27.5(14)	-7.7(14)	6	10.6(20) ^g
4^+	1666.559(60)	752	914.810(50)	10010(90)	29.9(11)	-4.0(18)	4	8.7(39) ^g
6^+	2669.806(80)	1667	1003.240(50)	6990(50)	27.7(12)	-5.1(15)	7	11.5(52) ^g
5^-	2705.609(70)	2344	(371.869) ^h	<40			3	<100
		2042	(663.713) ⁱ	<10				
[5]	3016.857(80)	1667	1039.037(30)	2480(30)	-26.7(11)	2.4(16)	3	<20
[5,6]	3029.545(90)	2706	311.248(30)	112(8)	35(11)	0	2	
		2670	359.719(40) ^j	25(5)				
		2042	(987.643) ^k	<25				
6^-	3271.945(80)	1667	1363.134(60)	135(15)	35(10)	16(13)	4	
8^+	3298.357(80)	2706	[566.347(40)]	350(10)	-54(4)	4(5)	4	
7^-	3423.295(80)	2670	628.550(40)	6100(70)	26.5(8)	-4.0(9)	4	90(10);90(9) ^g
		2670	717.696(40)	1700(200)	24.9(15)	-2.8(20)	0	12(2)
8^+	3532.562(90)	2670	(753.487) ^l	<500			0	<5
		3298	234.205(15)	2640(50)	33.4(16)	2.6(21)	0	
		2670	(862.75) ^m	$\leq 420(40)$	15(11)	0	4	<10
[7]	3646.334(90)	3423	223.038(30)	350(10)	25.6(20)	-2.4(30)	4	
(8 ⁺)	3791.706(95)	3533	[259.943(25)]	190(6)	-45(7)	17(8)	2	
[8]	4133.65(12)	3423	[710.350(90)]	100(15)	-50(16)	0	1	
		3271	(861.70) ^m	$\leq 420(40)$	15(11)	-11(12)	5	3.0(6)
(10 ⁺)	4325.990(95)	3298	1027.626(30)	2700(50)	26.9(11)	-4.4(11)	4	13(4)
10 ⁺	4418.58(12)	3533	885.899(40)	2520(50)	26.0(17)	-4.2(21)	4	
		3298	[1120.457(80)]	320(10)	33(6)	-19(8)	6	
(9 ⁻)	4429.321(90)	3423	1006.019(60)	1250(30)	32(4)	-6(5)	2	11(2)
[11]	5233.59(16)	4419	815.00(10)	1350(30)	-26.7(17)	7(5)	2	18(8)
(11 ⁻)	5388.66(10)	4429	959.337(40)	670(10)	21(3)	3(3)	1	4(1)
(12 ⁺)	5396.36(18)	4419	977.955(50)	830(30)	23(4)	-3(5)	13	3.8(9)
		4326	1070.186(40)	2170(30)	19(3)	0(3)	3	
(12 ⁺)	5646.48(16)	4419	1227.90(30)	270(30)	-4(7)	7(10)	5	<2
[12]	5974.77(17)	5234	741.183(60)	490(80)	-39(6)	9(9)	7	6.1(10)
[13]	[6232.31(18)]	5234	998.719(90) ⁿ	710(70)	27(5)	-2(8)	0	7.5(9)
(14 ⁺)	6321.04(18)	5396	924.684(40)	1710(30)	30.1(10)	-5.0(13)	6	
[13]	[6339.81(32)]	5389	951.15(30)	580(50)	31(6)	-4(7)	9	<1.0 ^o
[14]	7015.29(21)	6321	694.25(10)	1800(200)	+25(5)	-3(7)	9	<1.5 ^o
[15]	7396.44(29)	7015	381.15(20)	900(100)	-44(3)	+4(6)	9	

TABLE IV. (Continued).

^aFrom Ref. 3 or speculations from the present results (square brackets).
^bCorrected for recoil. The uncertainty in the least significant figure is given in parentheses. E_i completely enclosed in parentheses are to some degree speculative.
^cNot corrected for recoil. Energies enclosed in parentheses are calculated from $E_i - E_j$. Those in square brackets were not positively identified in the $\gamma\gamma$ coincidence data and thus are somewhat uncertain. An entry of 0 for A_4 means the fit was to $I_\gamma(1 + A_4 P_2)$ only, i.e., χ^2 was not significantly improved by the inclusion of an A_4 term.
^dThe relative intensity I_γ is corrected for the relative γ -ray efficiency and is in arbitrary units.
^eRelative side feeding of the level in question in units of $100I_\gamma$.
^fFrom the RDM measurements unless otherwise noted.
^gFrom Ref. 8.
^hA γ ray of 362.584(80) keV with an intensity of 140(10) units of unknown origin was observed but not the 2705 \rightarrow 2343 transition of Ref. 3.
ⁱIn Ref. 3 a 663-keV transition was assigned to a 2705 \rightarrow 2042 transition. The branching ratio was not given.
^jObscured in singles by an unknown contaminant. E_γ and I_γ are from the β^+/EC results.
^kThe absence of this transition is evidence that one of the 3030-keV levels assigned to ^{86}Nb decay (Table I) is different from this 3030-keV level.
^lReported in Ref. 3 with no branching ratio given.
^mAn unresolved doublet with an average energy of 862.43(10) keV and an intensity of 420(40) units can have contributions from both the 3533 \rightarrow 2670 and 4134 \rightarrow 3271 transitions (Ref. 3). However, the excitation function for this doublet is not typical of the 2pn channel.
ⁿThe presence of a 1000 ± 2 keV γ ray somewhere above and feeding the 5234-keV level is definite; its placement here is not.
^oThis transition shows a Doppler shift. The analysis to obtain a lifetime is described in Ref. 2.

into the low-lying levels could be overlooked. The problem is quite severe in the present case since Q_{EC} is large enough to accommodate significant β^+/EC feeding of levels several MeV above those observed. In the present $\gamma\text{-}\gamma$ coincidence measurement a 2-MeV γ transition having $I_\gamma \simeq 20$ (units of Table I) would be on the threshold of perception. We indicate the error introduced by overlooking such a transition into each level by taking σ_- to be the root mean square of this error and the statistical uncertainty. Of course, it should be kept in mind that even more than one such feeding transition could be overlooked for a given level.

Using the presently measured Q_{EC} and $t_{1/2}$ values, we obtain the allowed $\log ft$ values of Table III. Most of the $\log ft$ values are small enough so that they are likely to correspond to allowed transitions, although only the decays to the two highest-lying levels and the 6^+ 2670-keV level meet the accepted criterion¹⁵ for exclusion of forbidden decay, i.e., $\log ft > 5.9$. Assuming all are allowed, the decays to the 4^+ and 6^+ levels would fix the ^{86}Nb ground state as 5^+ . This, however, leads to a discrepancy with the most probable spin-parity assignments for the 2042- and 2344-keV levels ($J^\pi = 3^+$ and 3^- , respectively) proposed by Hattula *et al.*³ Three possible explanations are evident:

(i) Both levels in question have $J^\pi = 4^+$. The extent of the disagreement of these latter assignments with the ($^3\text{He}, x\text{n}\gamma$) data is not clear from the presentation of Ref. 3.

(ii) There is an (undetected) low-lying isomer in ^{86}Nb , as in $^{88,90}\text{Nb}$, such that the intensities of Table I involve allowed contributions from the decay of two ^{86}Nb levels of different spin and/or parity. In this case, however, the two half-lives must be nearly identical, since there was no evidence for a different value of $t_{1/2}$ for the 2042- and 2344-keV levels ($\Delta t_{1/2} \leq 5$ s).

(iii) The most likely explanation is that the 2042- and 2344-keV levels are not fed in (β^+/EC) decay to any significant extent, and that the "apparent" (β^+/EC) branching is due to unobserved γ flux into these levels, as discussed previously. In any event, it is clear that more work must be done to establish a definitive decay scheme for ^{86}Nb .

B. In-beam $^{60}\text{Ni}(^{29}\text{Si}, 2\text{pn}\gamma)^{86}\text{Zr}$ studies

The in-beam high-spin investigation of ^{86}Zr consisted of γ -ray excitation functions, angular distributions, recoil distance (RDM) and Doppler shift attenuation (DSA) lifetime measurements, and $\gamma\gamma$ -coincidence measurements. A ^{29}Si beam of 10–50 particle nA (particle nanoamps) at $E(^{29}\text{Si}) = 70\text{--}120$ MeV was provided by the second stage of the BNL double MP tandem facility. The experimental procedures were nearly identical to those used in the in-beam study² of $^{88,90}\text{Zr}$ and therefore they will only briefly be discussed. Gamma rays were detected with both large coaxial Ge detectors and a planar low-energy photon spectrometer (LEPS). For the excitation functions, RDM, and angular distribution measurements one Ge detector was placed in a NaI(Tl) anti-Compton shield, the whole operating as a Compton suppressed spectrometer (CSS).

The γ - γ coincidences were measured using the CSS detector and two unshielded Ge detectors. The target consisted of a 1.1-mg/cm² ⁶⁰Ni foil which, in all but the RDM measurements, was backed by 13 mg/cm² of evaporated natural Pb. The excitation function was taken in 10-MeV steps from $E(^{29}\text{Si})=70$ to 120 MeV. The ⁸⁶Zr yield was found to peak near 100 MeV and so angular distribution, γ - γ coincidence, and RDM lifetime measurements were performed at that energy. These were all routine except that the excitation function and angular distribution measurements were made with a timer/programmer control set for a sequence with a 10-s beam on period during which prompt events were recorded followed by a 1-s beam off waiting period and a 1-s period for recording delayed events. This procedure was followed so that the prompt data could be corrected for any delayed contributions from β^+ /EC decay. It was important to do so since it turned out that delayed activities constituted a large fraction of the observed intensity near the bottom of the decay scheme and subtraction of these activities was necessary in order to obtain accurate angular distributions and excitation functions. The method used provided a quite accurate way of correcting for these activities as well as providing useful information on them.

Angular distributions were taken simultaneously with the CSS detector at angles of 0°, 22°, 30°, 45°, 60°, 69°, and

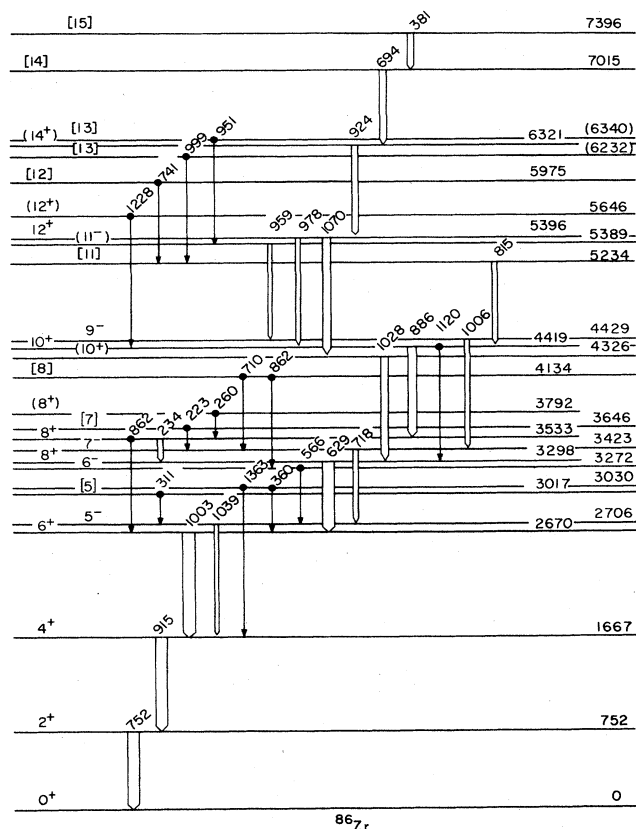


FIG. 3. Decay scheme of ⁸⁶Zr from the ⁶⁰Ni(²⁹Si,2pn γ)⁸⁶Zr reaction. The spin-parity assignments in square brackets are speculations based upon the present work. The remainder are those proposed in Ref. 3.

90° and the LEPS at angles of 90°, 97°, 105°, 120°, 135°, 140°, and 145°. A 31-h γ γ -coincidence measurement was recorded with three Ge detectors (one a CSS) and an \sim 6-h γ γ -coincidence measurement was performed with a LEPS-Ge combination to search for low-energy transitions. Recoil distance measurements (RDM) were made as described in Ref. 2. The recoil velocity in these measurements was $v/c=0.0257$.

A synthesis of the present measurements is given in Table IV from which we deduce the decay scheme of Fig. 3. The quality of the data (angular distributions, excitation functions, γ γ coincidences, etc.) is similar to that of Ref. 2 to which we refer the reader for an appraisal. The level lifetimes (mean lives) listed in Table IV are mostly from the RDM. Representative data are shown in Fig. 4. Only two γ rays definitely assigned to ⁸⁶Zr showed Doppler shifts in the angular distribution measurements. For these γ rays, limits on the lifetimes could be obtained using the Doppler shift attenuation method as discussed in Ref. 2. For both, the lifetimes are short enough so that the transitions must be predominantly dipole.

The decay scheme of Fig. 3 and Table IV is very similar to that of Hattula *et al.*³ with which we have no discrepancies. Our results proceed to slightly higher excitation energy via the 694-, 381-, and 959-keV transitions, while the results of Hattula *et al.* contain more information on the decay of nonyrast states. Spin-parity assignments based only on the present results are, in general, not very definitive. Two exceptions are the first two excited states for which firm $J^\pi=2^+$ and 4^+ assignments can be made. More definitive assignments for the other levels

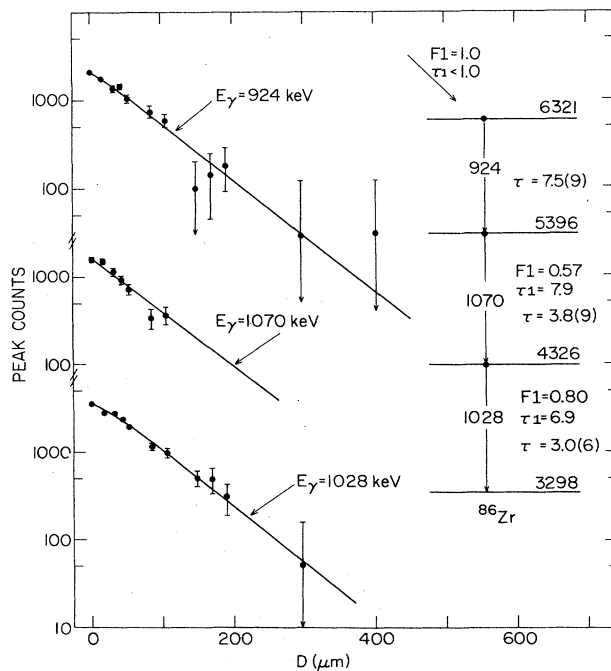


FIG. 4. Recoil distance lifetime results for the 6321-, 5396-, and 4326-keV levels of ⁸⁶Zr. The procedure is discussed in Ref. 2.

TABLE V. Transition rates and excitation energies in light, even zirconium isotopes. [The transition rates are in Weisskopf units (W.u.) as defined in Ref. 18.]

Nucleus	N	$E_x(2_1^+)$ (keV)	$B(E2; 2^+ \rightarrow 0^+)$ (W.u.)	$B(E2; 8^+ \rightarrow 6^+)$ (W.u.)
^{90}Zr	50	2186	5.38(17)	3.13(9)
^{88}Zr	48	1057	a	5.16(60)
^{86}Zr	46	752	14(3)	4.1(4)
$^{84}\text{Zr}^b$	44	540	40(2)	22(6)
$^{82}\text{Zr}^c$	42	407	86(10)	a

^aNot measured.

^bReference 19.

^cReference 1.

would be possible, if, as in the study² of $^{88,90}\text{Zr}$, linear polarization data were available. In Table IV and Fig. 3 we adopt the spin-parity assignments suggested by Hattula *et al.*³ with speculations from the present results given in square brackets. We caution that the assignments of Hattula *et al.*³ are not definitive.

The failure to observe higher-lying levels of appreciably higher spin in the reaction $^{29}\text{Si} + ^{60}\text{Ni}$ relative to $^{3,4}\text{He} + \text{Sr}$ was a major surprise. In contrast, the $^{88,90}\text{Zr}$ results from the reaction $^{18}\text{O} + ^{74,76}\text{Ge}$ reported in Ref. 2 extended the range of excitation energy over that observed in $^4\text{He} + \text{Sr}$ by ~ 4 MeV and extended the yrast levels from $J \sim 11$ to $J \sim 21$. Reaction calculations with CASCADE (Ref. 16) indicate the most probable spin formed in ^{86}Zr by $^{29}\text{Si} + ^{60}\text{Ni}$ is $\sim 16\hbar$ with a spread of $\sim 16\hbar$ FWHM (full-width at half maximum). The most probable explanation for our failure to find the decay of states above those observed is that in ^{86}Zr —in contrast to $^{89,90}\text{Zr}$ —the yrast levels in the range $J \sim 16$ – 24 decay by many different routes so that the intensities, being fragmented, are hard to detect. Clearly, a more sensitive experiment—such as the use of TESSA (Ref. 17) or some other total-absorption multiplicity detector—is needed to explore the higher-lying yrast levels in ^{86}Zr .

III. DISCUSSION: THE SYSTEMATICS OF THE EVEN, $A \leq 90$ Zr ISOTOPES

The excitation energies of the first $J^\pi = 2^+$ states in light Zr isotopes show a smooth decrease between ^{90}Zr and ^{82}Zr (Table V). The trend is reflected in a similarly regular increase in the $B(E2; 2 \rightarrow 0)$ values, as is also shown in Table V. However, it is probably incorrect to interpret these trends as being caused by a gradual onset of permanent deformation, as the $B(E2)$ values encompass contributions from static deformation and dynamic vibrations. A more useful indicator of the onset of permanent deformation is to examine the transition rates between higher-lying members of the yrast sequence where vibrational influences are smaller. Table V also gives the $B(E2)$ values for the yrast $8^+ \rightarrow 6^+$ decay for $^{84-90}\text{Zr}$. Here a new trend emerges with a jump in collectivity between ^{86}Zr and ^{84}Zr .

The suggestion that the onset of the nonspherical shapes is at $N=44$ for Zr isotopes is supported by the model potential energy surface calculations of Möller and Nix.²⁰ Between $A=90$ and 86 the nuclei are predicted to be spherical, but with a diminishing minima in the potential surface. At $A=84$ competition from nonspherical

TABLE VI. Transition strengths of some $E2$ transitions in ^{86}Zr .

Initial state ^a		Final state ^a		E_γ (keV)	τ (partial) ^b (ps)	$B(E2)^c$ (W.u.)	$B(E2; \text{rotor})$ (W.u.)
E_i (keV)	J_i^π	E_f (keV)	J_f				
752	2^+	0	0^+	752	10.6(20)	14(3) ^d	20
1667	4^+	752	2^+	915	8.7(39)	7(3) ^d	29
2670	6^+	1667	4^+	1003	11.5(52)	3.0(14) ^d	32
3298	8^+	2670	6^+	629	90(9)	4.1(4) ^d	34
4326	10^+	3298	8^+	1028	3.0(6)	10.5(21)	35
5388	11^-	4429	9^-	959	4(1)	11.1(28)	
5396	12^+	4419	10^+	978	14(3)	2.9(6)	35
5396	12^+	4326	10^+	1070	5.3(13)	4.9(12)	
6233	13	5234	11	999	6.1(10)	5.9(10)	
6321	14^+	5396	12^+	925	7.5(9)	7.1(9)	36

^aThe listed spin-parity assignments are assumed.

^bFrom the level lifetimes and branching ratios of Table IV.

^cThe transition strength in Weisskopf units (W.u.) as defined in Ref. 18.

^dFrom Ref. 8.

shapes starts and prolate shapes with $\epsilon_2 > 0.35$ are the most bound for $^{80,82}\text{Zr}$. Bonche *et al.*²¹ have done three-dimensional Hartree-Fock calculations for these nuclei. They find the mass quadrupole moment (in units of fm^2) $Q=0$ for both ^{90}Zr and ^{88}Zr .²¹ For ^{86}Zr they find that the energy surface is flat (for $0 < Q < 300$), while for ^{84}Zr a softly triaxial shape is indicated. Table IV is a collection of $E2$ transition rates measured for ^{86}Zr . The $2^+ \rightarrow 0^+$ transition shows some enhancement, probably indicating some softness to vibration, but amongst the higher states the transition strengths are only a few single particle units, and are similar to corresponding transitions in $^{88,90}\text{Zr}$. Hence, these data would appear to support a picture of excited states in ^{86}Zr arising from shell-model excitations of relatively few particles.

The interpretation of Hattula *et al.*³ is drastically different. They assume the nucleus has a permanently deformed shape and suggest that the excited states form rotational bands. Taking the deformation parameters from Hattula's work ($\epsilon_2=0.15$, $\epsilon_4=0$, $\gamma \approx -20$) and assuming a uniform charge distribution, the transition rates in the ground state band can be predicted in the framework of the rotational model. These are given in the last column of Table VI. It is clear that these predictions reproduce neither the trends nor the absolute values for any of the states with $J > 2$; therefore we feel that the interpretation and conclusions presented by Hattula *et al.*³ should be viewed with some caution.

Some further insight into the change in deformation of $Z \sim N \sim 40$ nuclei with neutron number is provided by the spins of the lowest-lying even-parity Nb levels. These levels are most simply generated by

$$\pi(g_{9/2})\nu(g_{9/2})^{A-81}.$$

Low-lying even-parity states with $0 \leq J \leq 9$ are expected, and which state lies lowest depends rather sensitively on details of the structure. The prediction²² of the spherical shell model gives correctly a lowest-lying even-parity state of 8^+ for ^{88}Nb and ^{90}Nb . For a highly deformed prolate nucleus and an inert (f,p) core, the simple Nilsson model prediction for the lowest-lying even-parity state is $J=(n+1)/2$, where $n=A-81$ is the number of $g_{9/2}$ neutrons. For ^{84}Nb , this prediction of 2^+ is consistent with a recent $^{84}\text{Nb}(\beta^+/\text{EC})^{84}\text{Zr}$ study²³ which indicates $J^\pi=1^+, 2^+$, or 3^+ . However, the prediction is expected to be modified by participation of the (f,p) core. Promotion of one or more pairs of (f,p) particles into the $g_{9/2}$ shell is expected, especially at high prolate deformations. This situation is handled quantitatively by Kreiner and Mariscotti²⁴ who applied a two-noninteracting-quasiparticle-plus-rotor model to $\tilde{\pi}g_{9/2} \times \tilde{\nu}g_{9/2}$ states in ^{76}Br . By analogy with this calculation one might expect a $J^\pi=3^+$ or 4^+ ground state for ^{84}Nb and $J^\pi=4^+$ or 5^+ for ^{86}Nb for reasonable prolate deformations. As discussed in Sec. II A, $J^\pi=5^+$ is suggested experimentally for ^{86}Nb .

This research supported at Brookhaven National Laboratory under the auspices of the U.S. Department of Energy, Division of Basic Energy Sciences, under Contract No. DE-AC02-76CH00016 and at Livermore Livermore Laboratory under Contract No. W-7405-ENG-48. One of us (C.J.L.) was also partially supported by a grant from the Science and Engineering Research Council (U.K.).

*Permanent address: University of Manchester, Manchester, England.

† Present address: Savannah River Laboratories, Aiken, SC 29801.

¹C. J. Lister, B. J. Varley, A. J. Irving, H. G. Price, and J. W. Olness (unpublished); C. J. Lister, Proceedings of the *International Symposium on In-beam Nuclear Spectroscopy* (The Hungarian Academy of Sciences, Drebecen, Hungary, 1984).

²E. K. Warburton, J. W. Olness, C. J. Lister, R. W. Zurmühle, and J. A. Becker, *Phys. Rev. C* **31**, 1184 (1985), preceding paper.

³J. Hattula, S. Juutinen, H. Helppi, A. Pakkanen, M. Piiparinen, S. Elfström, and Th. Lindblad, *Phys. Rev. C* **28**, 1860 (1983).

⁴J. W. Tepel, *Nucl. Data Sheets* **25**, 553 (1978).

⁵G. Korschinek, E. Nolte, H. Hick, K. Miyano, W. Kutschera, and H. Morinaga, *Z. Phys. A* **281**, 409 (1977).

⁶A. C. Rester, R. Gosselar, C. Günther, H. Hübel, J. Lange, L. Posthumus, J. Konijn, and B. Van Nooijen, *Proceedings of the International Conference on Nuclear Structure, Tokyo, 1977*, edited by T. Marumori (Physical Society of Japan, Tokyo, 1978), p. 305.

⁷J. E. Kitching, P. A. Batay-Csorba, C. A. Fields, R. A. Ristinen, and B. L. Smith, *Nucl. Phys. A* **302**, 159 (1978); C. A. Fields and F. W. N. de Boer, *Z. Phys. A* **311**, 127 (1983).

⁸M. Avrigeanu, V. Avrigeanu, D. Bucurescu, G. Constantinescu, M. Ivascu, D. Pantelica, M. Tanase, and N. V. Zamfir, *J.*

Phys. G **4**, 261 (1978).

⁹S. Della Negra, D. Jacquet, and Y. LeBeyec, *Z. Phys. A* **308**, 243 (1982).

¹⁰D. E. Alburger and T. G. Robinson, *Nucl. Instrum. Methods* **164**, 507 (1979).

¹¹C. J. Lister, P. E. Haustein, D. E. Alburger, and J. W. Olness, *Phys. Rev. C* **24**, 260 (1981).

¹²S. K. Saha, P. E. Haustein, D. E. Alburger, C. J. Lister, J. W. Olness, R. A. Dewberry, and R. A. Naumann, *Phys. Rev. C* **26**, 2654 (1982).

¹³C. J. Lister, B. J. Varley, D. E. Alburger, P. E. Haustein, S. K. Saha, J. W. Olness, H. G. Price, and A. D. Irving, *Phys. Rev. C* **28**, 2127 (1983).

¹⁴R. C. Pardo, C. N. Davids, M. J. Murphy, E. B. Norman, and L. A. Parks, *Phys. Rev. C* **15**, 1811 (1977); C. N. Davids, C. A. Gagliardi, M. J. Murphy, and E. B. Norman, *ibid.* **19**, 1463 (1979).

¹⁵S. Raman and N. B. Gove, *Phys. Rev. C* **7**, 1995 (1973).

¹⁶F. Pühlhofer, *Nucl. Phys. A* **280**, 267 (1977).

¹⁷P. J. Twin, R. Aryeainjad, D. J. G. Love, A. H. Nelson, and P. J. Nolan, *Nucl. Instrum. Methods* (to be published).

¹⁸S. J. Skorka, J. Hertel, and T. W. Retz-Schmidt, *Nucl. Data* **2**, 347 (1966).

¹⁹H. G. Price, C. J. Lister, B. J. Varley, W. Gelletly, and J. W. Olness, *Phys. Rev. Lett.* **51**, 1842 (1983).

²⁰P. Möller and J. R. Nix, *At. Data Nucl. Data Tables* **26**, 165

- (1981).
- ²¹P. Bonche *et al.* (unpublished); M. S. Weiss, private communication.
- ²²J. A. Becker and S. D. Bloom, private communications.
- ²³S. K. Saha, P. E. Haustein, R. A. Dewberry, and R. A. Naumann (unpublished).
- ²⁴A. J. Kreiner and M. A. J. Mariscotti, *Phys. Rev. Lett.* **43**, 1150 (1979).